Neutron-enhanced annealing of radiation damage formed by self-ion implantation in silicon

A. Kinomura,[a] A. Chayahara, Y. Mokuno, N. Tsubouchi, and Y. Horino
National Institute of Advanced Industrial Science and Technology (AIST), 1-1-1 Umezono, Tsukuba, Ibaraki 305-8568, Japan

T. Yoshiie, Y. Hayashi, and Q. Xu
Research Reactor Institute, Kyoto University, Kumatori-cho, Sennan-gun, Osaka 590-0494, Japan

Y. Ito, R. Ishigami, and K. Yasuda
Wakasa Wan Energy Research Center, 64-52-1 Nagatani, Tsuruga, Fukui 914-0192, Japan

(Received 20 December 2005; accepted 26 April 2006; published online 15 June 2006)

The annealing effect of neutron irradiation has been observed for radiation damage in self-ion implanted silicon. Si samples implanted with $(0.5–2)\times10^{15}$ Si/cm^2 were neutron irradiated at 400 °C with the total number of displacements of 8.8×10^{-3} dpa. A heavily disordered (not amorphized) sample clearly showed damage annealing enhanced by the neutron irradiation. The annealing efficiency (the ratio of annealed defects to atomic displacements) was calculated to be 1.3 defects/displacement. This annealing efficiency was compared with the results of previous ion beam annealing studies. © *2006 American Institute of Physics*. [DOI: 10.1063/1.2211927]

Ion implantation in semiconductors requires thermal annealing for crystalline recovery of radiation damage. However, previous studies on ion beam annealing reported that appropriate ion irradiation can reduce preexisting radiation damage.[1–6] Among such studies, ion-beam-induced epitaxial crystallization (IBIEC) of amorphous layers in Si has been intensively studied.[4–6] Crystallization rates of IBIEC were found to be linearly dependent on nuclear energy depositions or atomic displacements, indicating that IBIEC is driven by point defect formation. One of the unique features of IBIEC is the existence of reversal temperatures below which epitaxial crystallization turns to layer-by-layer amorphization.[4,5] The reversal temperatures were measured to be about 200 °C depending on ion mass and flux. On the other hand, electron-beam-induced epitaxial crystallization (EBIEC) of implantation-induced amorphous layers in Si has been also reported.[7,8] EBIEC was observed only for the electron energies that can induce atomic displacements.[7] Such observation was consistent with the model that IBIEC is driven by point defect formation. Nevertheless, temperature dependence of EBIEC was quite different. No reversal temperature was found and weak crystallization occurred even at cryogenic temperatures instead of amorphization.[7]

In view of different annealing behaviors under ion and electron irradiations, it is interesting to examine the irradiation of another high-energy particle neutron. In principle, primary knock-on atoms (PKAs) and their collision cascades formed by fast-neutron irradiation are similar to those by self-ion irradiation. However, monoenergetic ions from accelerators form closely located collision cascades at constant depths, while neutrons form mostly small and well-isolated collision cascades. Moreover, electrons used for EBIEC ($\leqslant$1 MeV) form isolated Frenkel pairs and do not form collision cascades in general. Therefore, different annealing behaviors are expected for different particles because of different initial distributions of point defects. Such comparisons can give us further insight on the mechanisms of the beam annealing. To date, there have been some reports on crystallization of Ge, SiC/Al, and $Ti_{1-x}B_x$ under neutron irradiation.[9–11] However, these studies reported limited results, which cannot be directly compared with the ion beam annealing. This study aims to investigate recovery (annealing) of radiation damage in ion-implanted Si under neutron irradiation and to compare its annealing behaviors with the previous results on ion beam annealing.[1–6]

A Czochralski-grown (100)-oriented Si (*n*-type, P-doped, 4–7 Ω cm) wafer was used as a starting material. Damage layers were formed by room-temperature (RT) implantation of Si^+ at 200 keV to ion fluences of 5×10^{14}, 1×10^{15}, and 2×10^{15} cm^{-2}. The damaged samples were then neutron irradiated for 75.7 h at 400 °C in Material Controlled Irradiation Facility of Kyoto University Reactor operating at 5 MW.[12] The nominal neutron flux was 3.8×10^{13} n/cm^2 s (9.4×10^{12} n/cm^2 s for neutron energies of >0.1 MeV). This irradiation facility has a neutron energy distribution of typical light-water reactors.[12] Irradiation temperature was controlled with stability of ±2 °C by a heater and two sets of thermocouples. For comparison, some of the damaged samples were thermally annealed in flowing Ar gas at 400 °C for the same time (76 h) as the neutron irradiation. The samples were characterized by Rutherford backscattering/channeling (RBS/C) with 2 MeV He ions generated mainly by the Wakasa-wan multipurpose accelerator with synchrotron and tandem (W-MAST).[13] A scattering angle of RBS/C analysis was 140°. Depth scales were calculated based on stopping powers for random directions. Atomic displacements formed by neutrons and ions were evaluated by the SPECTER code[14] and the SRIM-2003 code,[15] respectively, with a displacement energy of 13 eV.

Figure 1 shows the RBS/C spectra for the sample implanted to a fluence of 2×10^{15} cm^{-2}. An amorphous layer was formed close to the surface. The spectra for the neutron-irradiated (closed circles) and thermally annealed (open circles) samples show that the fringes of the amorphous layer were recrystallized. It appears that the neutron-irradiated

[a]Electronic mail: a.kinomura@aist.go.jp

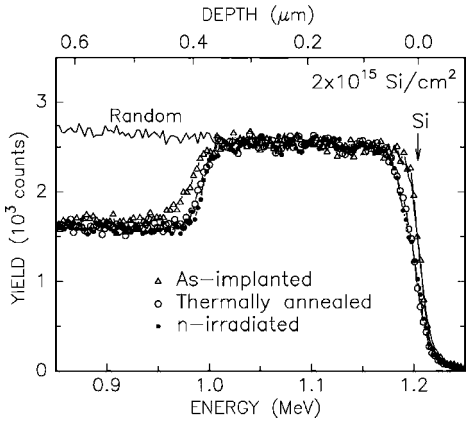

FIG. 1. RBS/C spectra of the amorphized sample after neutron irradiation (closed circles) and thermal annealing (open circles) at 400 °C, together with the spectrum of the as-implanted sample (triangles).

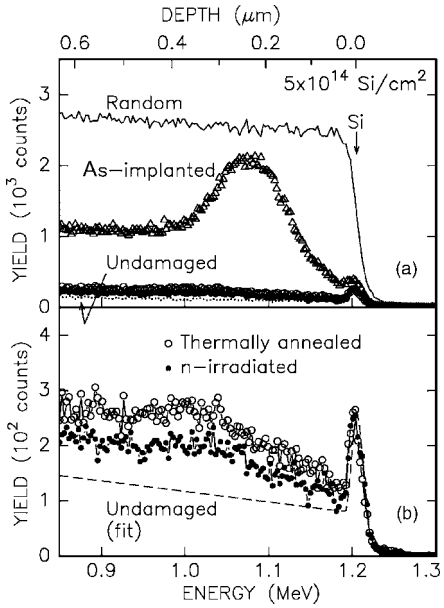

FIG. 2. RBS/C spectra of the heavily disordered sample after neutron irradiation (closed circles) and thermal annealing (open circles) at 400 °C, together with the spectrum of the as-implanted sample (triangles). (a) All the spectra. (b) Enlarged spectra for the annealed samples.

sample was annealed more than the thermally annealed sample. However, the difference between two spectra was very small. According to the SPECTER calculation, the total number of displacements by the neutron irradiation is 8.8×10^{-3} dpa. On the other hand, the typical number of displacements required for IBIEC at 400 °C in Si is close to 1 dpa to induce the interface motion which can be detected with a depth resolution of RBS/C analysis (about 300 Å at the surface) in this study.[6] It means that neutron-induced epitaxial crystallization like IBIEC was difficult to detect under the current experimental condition. Presumably, the difference between the neutron-irradiated and the thermally annealed samples is ascribed to the recovery of incompletely amorphized regions remaining near the amorphous/crystalline interfaces. A similar result was obtained for the amorphous layer formed by implantation of 1×10^{15} cm^{-2}.

Figure 2 shows the RBS/C spectra for the sample implanted to a fluence of 5×10^{14} cm^{-2}. A damage peak of the as-implanted sample did not reach the random level, as shown in Fig. 2(a). The implanted layer was heavily disordered but not fully amorphized. The scattering yield decreased close to the undamaged level after the irradiation or thermal annealing. In Fig. 2(b), the peak height of the neutron-irradiated sample is lower than that of the thermally annealed sample. It clearly indicates the damage annealing enhanced by neutron irradiation. It should be noted that thermal annealing for shorter time (400 °C, 8 h) or at higher temperature (450 °C, 75.7 h) gave the RBS/C spectra in agreement with the thermal annealing spectrum in Fig. 2 (400 °C, 76 h), indicating that the thermal recovery of disorder was well saturated. Disorder profiles were calculated for the neutron-irradiated and the thermally annealed samples after subtracting dechanneling contributions. Defects annealed by neutron irradiation (i.e., the difference in disorder between the neutron-irradiated and the thermally annealed samples) were 0.011 defects/atom at the damage peak. Note that "defects" mean, in this case, atoms displaced from lattice sites and defect states were not taken into account.

The annealing efficiency (i.e., the ratio of annealed defects to atomic displacements) of the heavily disordered sample, corresponding to Fig. 2, was calculated to be 1.3 defects/displacement. For comparison, annealing efficiencies were also calculated for previous studies on ion beam annealing in Si, as shown in Table I. Ion beam annealing of heavily disordered (not amorphized) samples exhibits saturation with increasing ion fluence.[1] It suggests that various types of defects coexist in damage layers, where simple defects can be easily annealed out but complex defects are annealed more slowly. The "annealing stage" in Table I refers to such behaviors. The annealing efficiencies measured at the "initial" stage are higher than those of the "saturated" stage and eventually getting lower with increasing ion flu-

TABLE I. Efficiencies of neutron-enhanced annealing compared with ion beam annealing.

Particle	Energy (keV)	Temperature (°C)	Annealing stage	Displacement rate (dpa/s)	Ionization (eV/displacement)	Efficiency (defects/displacement)	Reference
n	Fission	400	Not clear	3.2×10^{-8}	$(<3 \times 10^{3})$	1.3	This study
H^+	50	RT	Initial	7×10^{-5}[a]	1.2×10^{4}	$\leqslant 0.07$[b]	1
He^+	50	RT	Initial	1×10^{-3}[a]	8.7×10^{2}	$\leqslant 0.05$[b]	1
Si^+	1250	RT	Not clear	4×10^{-4}	8.4×10^{2}	0.04[b]	2
Ne^+	80	250	Saturated	7×10^{-4}	7.0×10^{1}	$\geqslant 0.5$[c]	3

[a]A beam current density of 5 μA/cm^2 was assumed.
[b]Calculated from RBS/C yields.
[c]Calculated from areal densities of displaced atoms, assuming a damage-layer thickness as the full width at half maximum (FWHM) of its initial damage profile.

ence. In terms of the neutron-enhanced annealing, the current result is not enough to determine on annealing stages.

The neutron-enhanced annealing showed the highest annealing efficiency in Table I. Let us interpret this result in comparison with ion beam annealing. Firstly, the much lower displacement rate of the neutron irradiation may be responsible for the higher annealing efficiency. Secondly, the irradiation temperature was higher than those of the ion beam annealing experiments. An apparent displacement-rate dependence of the annealing efficiency can be approximated by an nth pseudo-order function[16] as

$$\xi_0 = cr^n, \tag{1}$$

where c is a constant and r corresponds to the displacement rate. Unfortunately there has been no report on flux dependence of ion beam annealing for heavily disordered layers. Instead, three types of n values were examined: $n=-1/2$ (binary reactions of defects), $n=-1/4$ [a value proposed for IBIEC (Ref. 17)], and $n=0$ (no displacement-rate dependence). Note that displacement-rate dependence for ion beam annealing of disordered layers is expected to be similar to that for IBIEC, if production rates of freely migrating defects dominate the crystalline recovery processes. We assume that the annealing efficiency ξ as a function of temperature T can be written with an apparent activation energy E as

$$\xi = \xi_0 \exp(-E/kT), \tag{2}$$

where k is the Bolzmann constant. Based on Eqs. (1) and (2), the efficiency of the ion beam annealing at 400 °C (3.2×10^{-8} dpa/s) can be extrapolated from the ion beam data in Table I. The estimated efficiencies were 1.6×10^2, 12, and 0.94 defects/displacement for $n=-1/2$, $-1/4$, and 0, respectively. It is difficult to draw a quantitative conclusion from this estimation because of several assumptions and uncertainties (especially originating from different annealing stages) in addition to the lack of data. However, it seems possible to evaluate the efficiency of the neutron-enhanced annealing in the same way as the ion beam annealing on condition that weak displacement-rate dependence and Arrhenius-like temperature dependence apply to this case.

The third possibility is the effect of electronic excitation (defect ionization). The ionization energy for the neutron-enhanced annealing in Table I was calculated from the absorbed gamma-ray energy, assuming average gamma-ray energy of 2 MeV.[18] The gamma-ray absorption occurs uniformly in samples, while ionization by ion beam irradiation occurs at highly localized regions along ion tracks. Therefore, the value in Table I may be overestimated in terms of defect ionization. Even if this value is acceptable, the ionization caused by the fission gamma rays was less than the ionization during the H ion irradiation in Table I. On the other hand, PKAs formed by neutron irradiation also cause ionization in the same way as self-ion irradiation. SRIM-2003 calculations showed that the ionization by these PKAs is of the order of 10 eV/displacement and it is less than the ionization by the ion irradiations in Table I. It is thus difficult to correlate the defect ionization with the higher annealing efficiency.

Atomic displacements can be generated by gamma rays as well as neutrons and they are not negligible if gamma-ray flux is very strong.[18] We roughly estimated atomic displacements by gamma rays based on the method using Mckinley-Feshbach cross sections,[19] assuming a gamma-ray energy of 2 MeV.[18] A displacement rate by gamma rays at the irradiation facility was about 1×10^{-10} dpa/s, while the displacement rate by neutrons was 3.2×10^{-8} dpa/s. Therefore, the displacements by gamma rays are negligible in this study.

The efficiency of the neutron-enhanced annealing was more than 1 (1.3 defect/displacement). It means that one displacement leads to annihilation of more than one defect. Since some of Frenkel pairs annihilate through interstitial-vacancy recombination without contributing to annealing, an actual annealing efficiency could be higher. We speculate that a point defect (vacancy or interstitial) gives rise to dissolution of a complex defect and released point defects annihilate with other point defects. Or another possibility is atomic displacements generated by subthreshold effects.[20] The displacement energy (13 eV) in this study was determined for crystalline Si. If actual displacement energies are reduced in damaged Si, the annealing efficiency becomes lower.

In conclusion, the annealing effect of fission-neutron irradiation at 400 °C was examined for radiation damage in Si samples implanted with $(0.5-2)\times10^{15}$ Si/cm^2. Atomic displacements given to the sample were insufficient to confirm epitaxial crystallization of amorphized layers. Neutron-enhanced annealing was clearly observed for a heavily disordered sample. The efficiency of neutron-enhanced annealing was calculated to be 1.3 defects/displacement.

This work has been carried out in part under the Visiting Researcher's Program of the Kyoto University Research Reactor Institute. The authors would like to thank K. Sato, Y. Nakano, K. Fujii, and R. Suzuki for their assistance on this study.

[1] W. H. Kool, H. E. Roosendaal, L. W. Wiggers, and F. W. Saris, Radiat. Eff. **36**, 41 (1978).
[2] O. W. Holland, Appl. Phys. Lett. **54**, 320 (1989).
[3] B. Zeroual and G. Carter, Nucl. Instrum. Methods Phys. Res. B **44**, 318 (1990).
[4] R. G. Elliman, J. S. Williams, W. L. Brown, A. Leiberich, D. M. Maher, and R. V. Kneol, Nucl. Instrum. Methods Phys. Res. B **19/20**, 435 (1987).
[5] F. Priolo and E. Rimini, Mater. Sci. Rep. **5**, 319 (1990).
[6] A. Kinomura, J. S. Williams, and K. Fujii, Phys. Rev. B **59**, 15214 (1999).
[7] G. Lulli and P. G. Merli, Phys. Rev. B **47**, 14023 (1993).
[8] D. Hoehl, V. Heera, H. Bartsch, K. Wollschläger, W. Skorupa, and M. Voelskow, Phys. Status Solidi A **122**, K35 (1990).
[9] J. R. Parsons and R. W. Balluffi, J. Phys. Chem. Solids **25**, 263 (1964).
[10] A. Kohyama, S. Sato, H. Tezuka, and M. Kondo, J. Nucl. Mater. **179-181**, 254 (1991).
[11] T. Shikama and H. Kayano, J. Nucl. Mater. **179-181**, 465 (1991).
[12] T. Yoshiie, Y. Hayashi, S. Yanagita, Q. Xu, Y. Satoh, H. Tsujimoto, T. Kozuka, K. Kamae, K. Mishima, S. Shiroya, K. Kobayashi, M. Utsuro, and Y. Fujita, Nucl. Instrum. Methods Phys. Res. A **498**, 522 (2003).
[13] S. Hatori, Y. Ito, R. Ishigami, K. Yasuda, T. Inomata, T. Maruyama, K. Ikezawa, K. Takagi, K. Yamamoto, S. Fukuda, K. Kume, G. Kagiya, T. Hasegawa, M. Hatashita, M. Yamada, H. Yamada, M. Dote, N. Ohtani, S. Kakiuchi, Y. Tominaga, S. Fukumoto, and M. Kondo, AIP Conf. Proc. **576**, 631 (2001).
[14] L. R. Greenwood and R. K. Smither, SPECTER neutron damage calculations for materials irradiations, Argonne National Laboratory, 1985.
[15] J. F. Ziegler, J. P. Biersack, and U. Littmark, *The Stopping and Range of Ions in Solids* (Pergamon, New York, 1985).
[16] M. Kiritani, J. Nucl. Mater. **169**, 89 (1989).
[17] V. Heera, R. Kögler, W. Skorupa, and R. Grötzschel, Nucl. Instrum. Methods Phys. Res. B **80/81**, 538 (1993).
[18] L. E. Rehn and R. C. Birtcher, J. Nucl. Mater. **205**, 31 (1993).
[19] O. S. Oen and D. K. Holmes, J. Appl. Phys. **30**, 1289 (1959).
[20] J. Bourgoin and M. Lannoo, *Point Defects in Semiconductors II* (Springer, Berlin, 1983).